Georgia Institute of Technology
Office of Sponsored Program
OSP Initiation -Deliverable Schedule
Report Generated on: 1/4/2007 12:47

Doc ID #: 103541
Old Project Number:
P/S Project Number: 25066RA
Rev #: INIT Mod #:
Initial Revision Completion Date: 30-AUG-06

Doc ID #: 103541

Sponsor: NAVY/NAVAL UNDERSEA WARFARE CTR/RI

Award Document: CONTR

Contract #: N66604-06-M-3150 **Contract thru:** GTRC

Project Director(s):

PDPI LYNCH, CHRISTOPHER S

Unit: MECH ENGR **Initiation Date:** 08-JUN-2006

Termination Perf Date: 07-DEC-2006 (Performance)

Termination Rpts Date: 07-DEC-2006

Project Title: DEVELOPMENT OF A MODEL FOR PREDICTING HEATING OF TRANSDUCER DEVICES

Note: Deliverables sorted on 'Due Date to Sponsor' column

Rev No(1)	Description of Deliverable (2)	Deliv Id No	Period Covered		Due Date to Sponsor (3)	Copies Req	Date Mailed (4)	Sat
*0	FINAL REPORT	1	08-JUN-2006	07-DEC-2006	07-DEC-2006	1	04 Jan 07	N

Total Count:1

* Satisfied

PLEASE NOTE:

1.An asterisk denotes this deliverable was changed or added by the mod.
2.The Deliverable Id No will remain associated with its originally assigned deliverable for the duration of the project.
Modifications to the project will no longer cause this number to be sequentially renumbered.
3.Blanks in the 'Due Date to Sponsor' indicate 'as appropriate' or 'as required'.
4.Blanks in 'Date Mailed' indicate that neither delivery nor notification of delivery has been accomplished through OSP/CSD.

Prepare reports in accordance with:

Please review the schedule for accuracy and contact the CO if changes are necessary.

Loss and Heat Generation in Piezoelectric Transducers

1 Introduction

Heat generation is one of the most important issues in piezoelectric devices working at high frequency such as resonant motors. It is caused by both electrical and mechanical losses in ferroelectric materials. The electrical and mechanical loss tangents were found to be proportional to each other (Hardtl 1982). The losses below the Curie temperature are mainly caused by domain wall movements. Models relating the losses and heat generation to field strength, frequency and temperature are needed.

To achieve certain vibration displacement/velocity, the amplitude of the driving electric field will be a function of frequency. Heat generation at low frequency (high electric field, low stress) is caused mainly by dielectric loss (D-E hysteresis loss), while at resonance (low electric field, high stress) it is mainly caused by mechanical loss (T-S hysteresis loss) (Uchino and Hirose, 2001; Uchino et al., 2000; Uchino et al., 2006).

Hysteresis is a lag between cause and effect. When hysteresis occurs with extensive and intensive variables, a hysteresis loop is formed. The work done on the system in a cycle is the area within the hysteresis loop of the extensive and associated intensive variables. This work is the energy loss, which is converted into heat (or other form of energy).

Field and stress induced domain-wall activities also lead to great changes of dielectric and piezoelectric constants (Hall, 2001; Zhang et al., 1994). A Rayleigh relationship was found between the permittivity of ferroelectrics and the ac electric field (Taylor and Damjanovic, 1997, 1998). It was shown that the permittivity decrease linearly with the logarithm of the frequency of the ac field. Similarly, at low alternating stress amplitudes, the relation of piezoelectric coefficient and stress may be described by the Rayleigh law, see Figure 1 (Damjanovic, 1997; Damjanovic and Demartin, 1996; Damjanovic and Demartin, 1997). The nonlinear response of piezoelectric ceramics was shown to obey the Rayleigh law in a specific field and low frequency ranges (Eitel et al., 2006).

It is a great challenge to accurately model the hysteretic loss in piezoelectric actuators under dynamic loadings (Hall, 2001). Models for the nonlinear behavior of the ferroelectric materials under the combined electric field and stress are needed for the simulation of the electric field and stress distributions in piezoelectric components. At small alternating stress and electric field of certain ranges, complex material constants may be used to simulate the hysteretic response. For arbitrary loadings and loading paths, micro-mechanical models based on domain switching and domain wall motion should be a better solution.

Here we report our attempts in modeling the losses and heat generation as functions of field strength, frequency and temperature. Details of the model is described and discussed below.

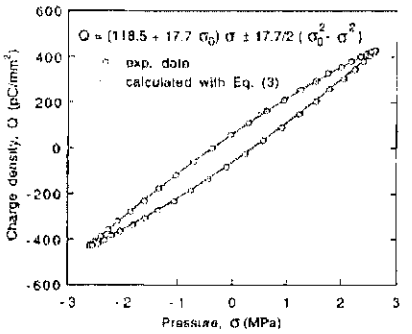

Figure 1. Rayleigh law for piezoelectric and dielectric coefficients (Damjanovic 1997)

2 Transducer and Material Loss Modeling

2.1 Transducer Model and Solution Scheme

A basic resonant transducer contains a piezoelectric stack, a head mass and a tail mass, as shown in Figure 2(a). When it is fixed at some position of the stack, u = 0 at x = 0, it can be simplified as shown in Figure 2(b). More complex transducer design may be considered by through dynamics analysis.

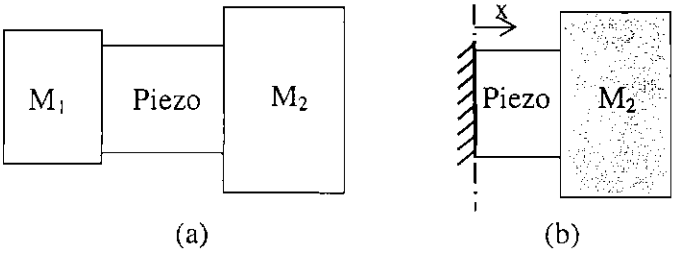

Figure 2. Sketch of piezoelectric transducer

To model the losses and heat generation of such a transducer, the following steps are taken:

1. Analyze the dynamics of transducer structure. Start with linear analysis, Evaluate the electric field E induced displacement u and stress T as functions of frequency f.

2. Compute losses in a field cycle as functions of electric field E, Stress T, frequency f and temperature. Develop models to compute the losses in a field cycle. This is the main task of the project. It includes material hysteresis modeling and implementation of material models for the dynamics system of transducers. The contributions of electric field and stress to losses are the main concern. The effects of frequency and temperature may be put in through frequency and temperature dependent parameters.

3. Compute temperature increase due to heat generation. The temperature increase profile of the transducer may be computed when the total losses and overall heat transfer coefficient is known.

2.2 Dynamics of Transducer Structure (Linear Solution)

Piezoelectric stack data:

```
V =10*10*3*1e-9; Area=320e-6; den=8000; c=420; % (Powers 00)
ve= 8*8*2.8e-9;      % ve: effective (piezo) volume
A = 8*8e-6;          % cross Area
L = 1.4e-3;          % stack length
k = 150;             % Heat transfer coefficient, overall
M = 0.1;             % tail mass
```

Piezoelectric coefficients:

```
dd1:=2000e-12: ss1:= 60e-12; ee1:=5000*e0;  # PMN-PT
```

Loss tangents:

```
ad=0.1: as=0.1: ae=0.1:
```

Field variable:
E – electric field (bias E_0, amplitude E_a)
Dele – electric displacement
S – strain
T – stress. (bias/preload T_0, amplitude T_a)
w/ω – angular frequency
f – frequency
t – time

Driving electric field:

$$E := t \to E0 + Ea \sin(w\, t)$$

Governing equations:

$$pde := den\left(\frac{\partial^2}{\partial t^2} u(x, t)\right) = \frac{\partial}{\partial x} T(x, t)$$

$$T := \frac{S - dd1\, E}{ss1}$$

$$S := \frac{\partial}{\partial x} u(x, t)$$

Boundary conditions:
Left end:

$$u(0, t) = 0$$

Right end:

$$T2 := T0 - \frac{F2}{A}$$

$$F2 = M\left(\frac{\partial^2}{\partial t^2} u(L, t)\right)$$

Solution
Displacement:

$$u := (x, t) \rightarrow (ss1\ T0 + dd1\ E0)\, x + ua \sin(wv\ x) \sin(w\ t)$$

$$ua := \frac{dd1\ A\ Ea}{\cos(wv\ L)\ wv\ A - ss1\ M\ w^2 \sin(wv\ L)}$$

$$wv := w\ vs \qquad vs := \sqrt{den\ ss1}$$

,

Resonant frequency:

$$w1 := 0, \frac{\text{RootOf}(-\_Z\ M \tan(\_Z) + L\ A\ den)}{\sqrt{den\ ss1}\ L}$$

(transcendental frequency equations)

$$Ea := -\frac{ua\ (-\cos(wv\ L)\ wv\ A + ss1\ M\ w^2 \sin(wv\ L))}{dd1\ A}$$

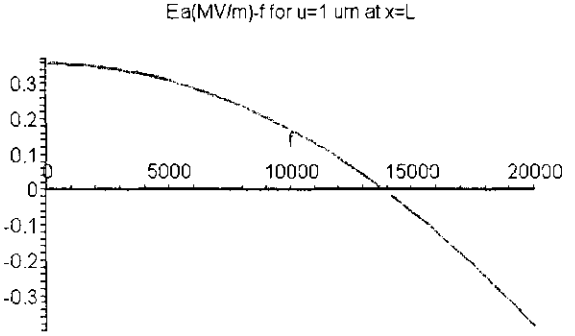

Figure 3. Ea (f) to achieve u = 1 μm at x = L. resonant frequency $\omega_1 \cong 14$ kHz

Strain:

$$S := (x, t) \rightarrow ss1\ T0 + dd1\ E0 + ua \cos(wv\ x)\ wv \sin(w\ t)$$

Stress:

$$T := (x, t) \rightarrow \frac{ss1\ T0 + ua \cos(wv\ x)\ wv \sin(w\ t) - dd1\ Ea \sin(w\ t)}{ss1}$$

Electric displacement:

$$Dele := \frac{dd1\ (ss1\ T0 + ua \cos(wv\ x)\ wv \sin(w\ t) - dd1\ Ea \sin(w\ t))}{ss1} + ee1\ (E0 + Ea \sin(w\ t))$$

2.3 Computation of Work and Loss

Experiments on relaxor single crystals were performed in which the strain and electric displacement were varied. This experimental data can be integrated along the loading path to obtain the sum of the change of internal energy and the heat removed.

The energy balance of a unit volume can be expressed in an incremental form as

$$dE = \sigma_{ji} d\varepsilon_{ij} + E_j dD_j + dq$$

where the last term on the RHS is the thermal energy added per unit volume by heat flux. (Note the sign change since heat flux is outward positive. Also note that dq is an increment of heat added, not flux.)

The mechanical work along a loading path is given by

$$\Delta W^m = \int_A^B \sigma_{ij} d\varepsilon_{ij}$$

And the electrical work is

$$\Delta W^e = \int_A^B E_j dD_j$$

The energy equation becomes

$$\Delta E = \Delta W^m + \Delta W^e + \Delta q$$

In integrating a closed cycle under isothermal condition, the final state is the same as the initial state, i.e. $\oint dE = 0$. Since the integration is performed about a closed cycle, any offset at the end of the cycle is given by

$$\oint dW^m + \oint dW^e = -\Delta q$$

The mechanical and electrical work may be partitioned into a reversible part and an irreversible part. The reversible work for a closed cycle is zero, therefore the integrations gives the irreversible work (loss) in a cycle. They equal to the areas of the D-E loop and the T-S loop. The loss is converted into heat, which leads to temperature increase of the single crystal. Details on the thermodynamics of electromechanical coupled materials are given in Appendix A in the end of this report.

3 Complex Coefficient Model

3.1 Complex Constants

The ferroelectric constitutive relations can be expressed as:

$$\varepsilon_{ij} - \varepsilon_{ij}^{r} = S_{ijkl}^{E}\sigma_{kl} + d_{nij}E_{n}$$
$$D_{m} - D_{m}^{r} = d_{mkl}\sigma_{kl} + k_{mn}^{\sigma}E_{n}$$

The remnant strain and remnant electric displacement represent the nonlinearity and the irreversibility. The coefficients should also be field dependent. When the hysteresis is small, the relations can be expressed in complex form:

$$\varepsilon^{*}_{ij} = S_{ijkl}^{E^{*}}\sigma^{*}_{kl} + d^{*}_{nij}E^{*}_{n}$$
$$D^{*}_{m} = d^{*}_{mkl}\sigma^{*}_{kl} + k_{mn}^{\sigma^{*}}E^{*}_{n}$$

In which complex dielectric, elastic and piezoelectric constants are used.

Consider a steady electric field at frequency $f = \omega/2\pi$:

$E = E_a\mathrm{Cos}(\omega t)$

It can be expressed in complex form as

$E^* = E_a e^{I\omega t}$ ($E = \mathrm{Re}(E^*)$)

When the hysteresis is relatively small, the induced electric displacement can be expressed as

$D = D_a\mathrm{Cos}(\omega t - \delta)$

or in complex form

$D^* = D_a e^{I(\omega t-\delta)}$ ($D = \mathrm{Re}(D^*)$)

Where δ is the phase delay.

At zero stress state, the relation between D* and E* can be expressed as

$D^*=\varepsilon^*E^*$

Where ε^* is the complex dielectric constant

$\varepsilon^* = \varepsilon' - I\,\varepsilon'' = Da/Ea\ e^{-I\delta} = Da/Ea\ (\cos\delta - I\sin\delta)$

where

ε' is the real part of the dielectric constant; ε'' is the imaginary part of the permittivity, which is related to the rate at which energy is absorbed by the medium (converted into thermal energy, etc).

The loss tangent is the ratio of the imaginary permittivity to the real permittivity of a material.

$\tan\delta = \varepsilon''/\varepsilon'$

The complex elastic constant is analogous to the complex dielectric constant:

$s^* = s' - I\,s''$

where

s' is the real part, s'' is the imaginary part (loss modulus), $I^2 = -1$. They are related to the mechanical phase angle. Consider the stress-strain relation with phase angle δm:

Stress $T^* = T_a e^{I\omega t}$

Strain $S^* = S_a e^{I(\omega t - \delta m)}$

The dynamic elastic constant is

$s^* = S^*/T^* = S_a/T_a\, e^{-I\delta m} = S_a/T_a\,(\cos\delta_m - I\sin\delta_m) = s_1 + I\,s_2 = s_1(1 + I\tan\delta_m)$

$\tan\delta_m = s_2/s_1$. $s_1 \cong s$ (static constant) when $\tan\delta_m \leq 0.2$.

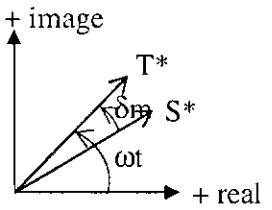

Figure 4. Complex variables and phase angle.

Similarly the complex piezoelectric constant is

$d^* = d' - I\,d''$

The coefficients are actually field dependent. They can be expressed as polynomials of applied stress and electric field amplitude.

3.2 Losses in Ferroelectrics

In ferroelectric materials there are dielectric loss and mechanical loss when electric field and stress are present. Under loadings (in complex form)

$E^* = E_a e^{I\omega t}$, or $cE := Ea\, e^{(I\, w\, t)}$

$T^* = T_a e^{I(\omega t+\delta T)}$, or $cT := Ta\, e^{(I\, w\, t)}\, e^{(I\, aT)}$ (with a phase difference δ_T to E)

The induced complex strain and complex electric displacement are:

$$cS := (s1 - I\, s2)\, Ta\, e^{(I\, w\, t)}\, e^{(I\, aT)} + (d1 - I\, d2)\, Ea\, e^{(I\, w\, t)}$$

$$cD := (d1 - I\, d2)\, Ta\, e^{(I\, w\, t)}\, e^{(I\, aT)} + (e1 - I\, e2)\, Ea\, e^{(I\, w\, t)}$$

In the above equations $(s1 - I\ s2)$ is the complex elastic constant, $(e1 - I\ e2)$ is the complex dielectric constant, and $(d1 - I\, d2)$ is the complex piezoelectric constant.

Assuming constant coefficients, Integration following Section 2.3 gives the electrical loss energy in a cycle:

$$Le := Ea^2\, e2\, \pi - Ta \sin(aT)\, Ea\, d1\, \pi + Ta \cos(aT)\, Ea\, d2\, \pi$$

This is the area of the D-E loop.

The mechanical loss energy in a cycle is

$$Lm := \frac{1}{2}\cos(aT)^2\, Ta^2\, s1 + \frac{1}{2}\sin(aT)^2\, Ta^2\, s1 + Ta^2\, s2\, \pi - \frac{1}{2}\, Ta^2\, s1 + Ta \sin(aT)\, Ea\, d1\, \pi$$

$$+ Ta \cos(aT)\, Ea\, d2\, \pi$$

This is the area of the T-S loop.

Total loss in a cycle:

$$Loss := \frac{1}{2}\cos(aT)^2\, Ta^2\, s1 + \frac{1}{2}\sin(aT)^2\, Ta^2\, s1 + Ta^2\, s2\, \pi - \frac{1}{2}\, Ta^2\, s1 + 2\, Ta \cos(aT)\, Ea\, d2\, \pi + Ea^2\, e2\, \pi$$

Figure 5 plots the total loss as a function of δ_T. The loss is maximum when T and E are in phase and minimum when T and E are with phase angle π. Phase angles must be regulated so that the total loss > 0.

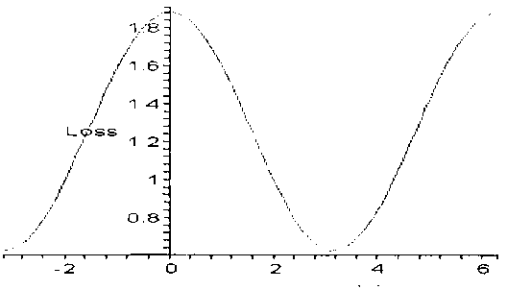

Figure 5. Loss as a function of δ_T.

When $\delta_T = 0$:
Mechanical work (loss) in a cycle (including coupling terms):

$$Lm := Ta^2\, s2\, \pi + Ta\, Ea\, d2\, \pi$$

Dielectric work (loss) in a cycle (including coupling terms):

$$Le := Ta\, Ea\, d2\, \pi + Ea^2\, e2\, \pi$$

Total work (loss) in a cycle:

$$Loss := Ta^2\, s2\, \pi + 2\, Ta\, Ea\, d2\, \pi + Ea^2\, e2\, \pi$$

3.3 Determination of Loss Tangents

According to the equations shown in last section, the losses in a cycle are functions of loss modulus as well as stress and electric field.

From experimental data, the losses can be obtained by computing the areas of the T-S loop and/or the D-E loop. When a Rayleigh relationship can be used to describe the T-S curve and/or the D-E curve, it can be used for the computation of the losses (Damjanovic, 1997). The effective loss modulus and loss tangents can then be computed from the losses.

There are different arguments regarding the relations of tan δe, tan δm and tan δp. It's more reliable to measure these values directly. The elastic loss modulus s'' can be measured under mechanical loading under constant electric field ($E_a = 0$),

$$s'' = \frac{L_m}{\pi T_a^2},\ \tan \delta_m = s''/\, s'$$

The dielectric loss modulus ε'' can be measured under electrical loading under constant stress ($T_a = 0$),

$$\varepsilon'' = \frac{L_e}{\pi E_a^2},\ \tan \delta e = \varepsilon''/\, \varepsilon'$$

The piezoelectric loss modulus d'' can be measured under combined stress and electrical loading (for simplicity of expression, consider the case the stress and electric field are in phase, $\delta_T = 0$),

$$d'' = \frac{Loss - \pi s'' T_a^2 - \pi \varepsilon'' E_a^2}{2\pi T_a E_a}, \tan \delta_p = d''/d'$$

Constant stress condition at high frequency is often not practical, therefore two tests of combined loadings with different stress and electric fields may be conducted, d'' and ε'' are then obtained by solving two equations of d'' and ε''.

It can also be measured from the S-E curve (at constant stress) or the T-D curve (at constant electric field) (Eitel et al., 2006),

$$d'' = \frac{A_{S-E}}{\pi E_a^2}, \quad d'' = \frac{A_{T-D}}{\pi T_a^2}$$

The loss tangents are functions of field frequency. Therefore measurements of loss tangents at different frequencies (particularly working frequencies) are needed. It has been observed that the piezoelectric loss tangents in hard and soft PZT decrease linearly with the logarithm of the frequency (Damjanovic, 1994; Damjanovic et al., 1996). Assuming such a relation, loss tangent data at a number of frequencies will be sufficient.

3.4 Simulation of the Dynamic Response

Apply stress T0 = -10 MPa, electric field E = E0 + Ea*sin(f*2*Pi*t), E0 = 0.5 MV/m. Ea is adjusted to achieve displacement u = 1 μm at x = L.

All the field variables can be computed as functions of position (x) and time (t). Work rate done by the electric field and the stress are

$$\int_0^L A\, T(x, t)\, dS(x, t)\, dx \qquad \int_0^L A\, E(x, t)\, dD(x, t)\, dx$$

The sum of them is the total work rate. Time integral of the work rate gives the work (and the loss).

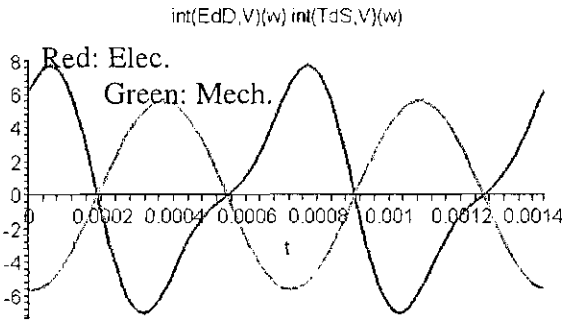

Figure 6. Electrical and mechanical work rate

In the following the results at three frequencies are compared:

1) At low frequency, f = 1.4 KHz, Ea = 0.35 MV/m
The induced stress is small. Loss in a cycle Loss1 = 0.16e-3 J

2) closer to resonance, f = 10 KHz, Ea = 0.17 MV/m
Large induced stress. Loss in a cycle Loss1 = 0.22e-3 J

3) Above resonance, f = 15 KHz, Ea = 0.06 MV/m
Large induced stress plus tensile stress. Loss in a cycle Loss1 = 0.24e-3 J

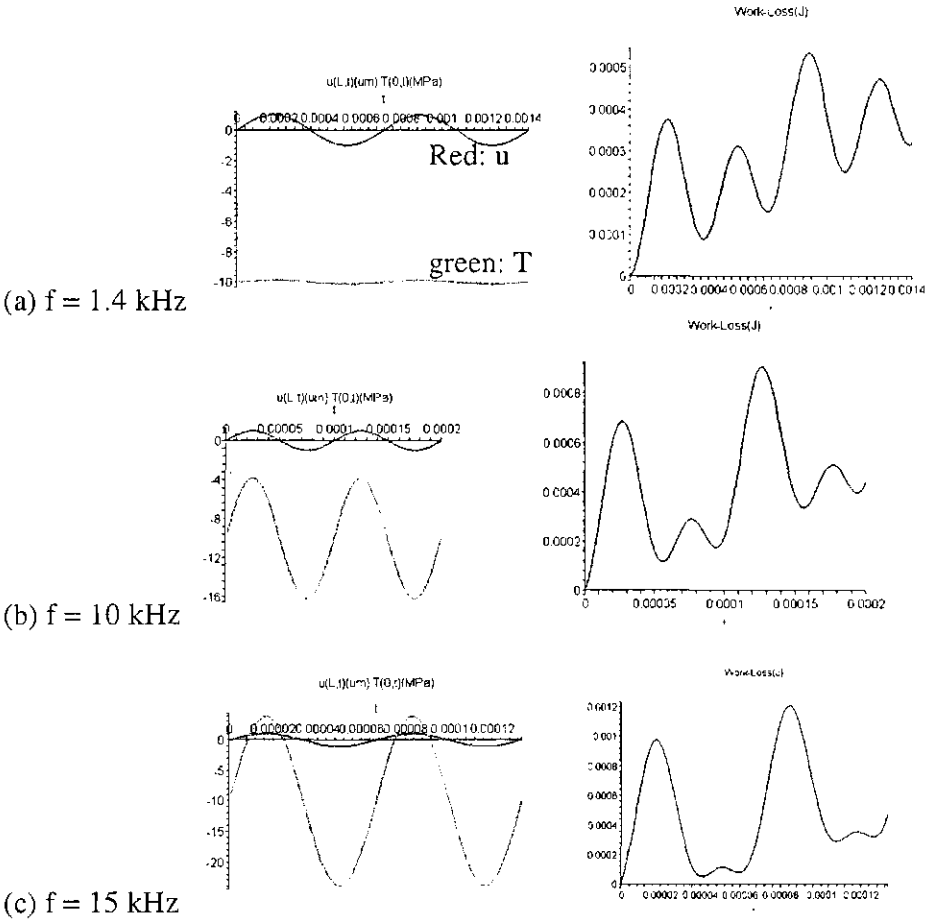

(a) f = 1.4 kHz

(b) f = 10 kHz

(c) f = 15 kHz

Figure 7. Left: u(L,t) and T(0,t); Right: work (and loss) as a function of time.

Loss tangents are functions of field (E, T, Temperature) and frequency. For illustration, here loss tangents are set to ad = 0.1, as = 0.1, ae = 0.1. Figure 8 and Figure 9 show the different D-E and S-E curves for frequency below resonance and above resonance.

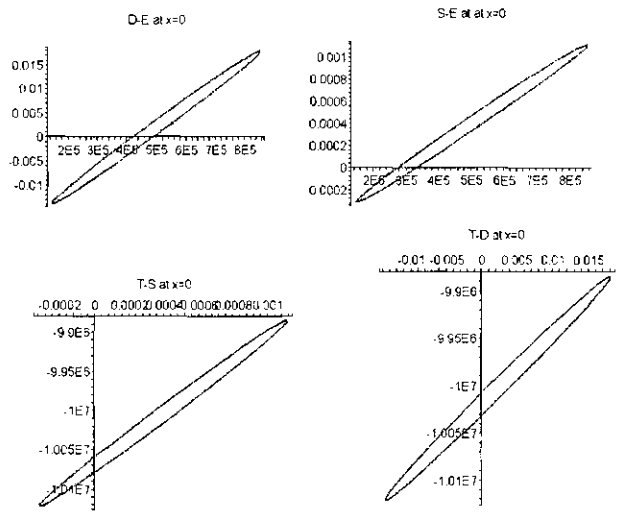

Figure 8. At f = 1.4 kHz, u, S, T, D and E are in-phase

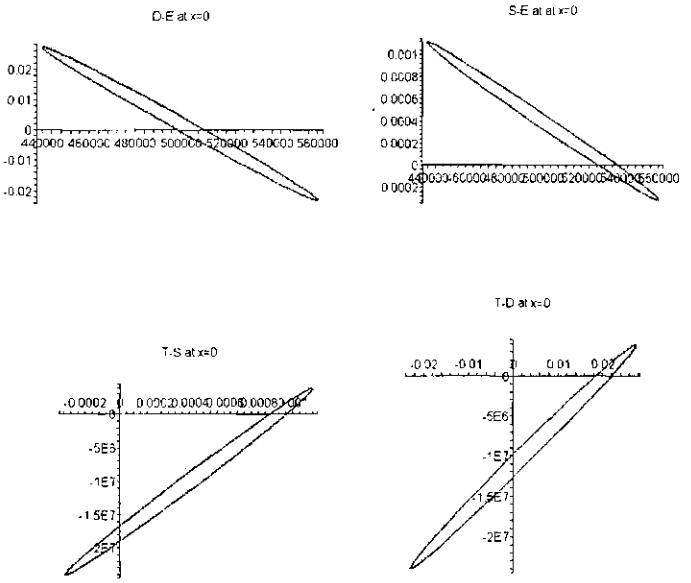

Figure 9. At f = 15 kHz, u, S, T, D and E are anti-phase

For the current transducer dimension and with the assumption of constant complex coefficients, the stress along the actuator is quite uniform. In such case, the strain/stress and electric displacement may be averaged as functions of time (t) only.

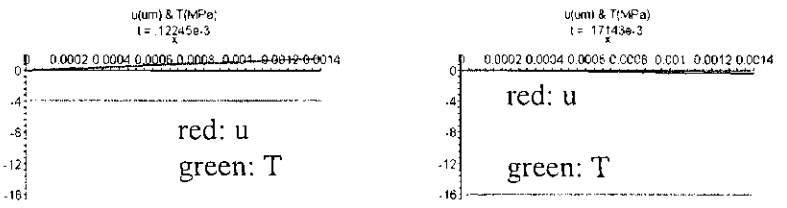

Figure 10. f = 10 kHz, u and T along the piezoelectric element when u(L) = ±1 μm.

3.5 Simulation with Simulink

The process may be simulated with Simulink. The current code simulates a lumped system (the distributed mass of the piezoelectric element is neglected). Parameters of the transducer, piezoelectric material coefficients and loss tangents are put in, and an electric field and stress preload are applied. Induced stress is connected as a feedback to satisfy the dynamic equation. Field variables, work done by the electric field and stress are computed and plotted as functions of time. The net work done in a cycle is the loss.

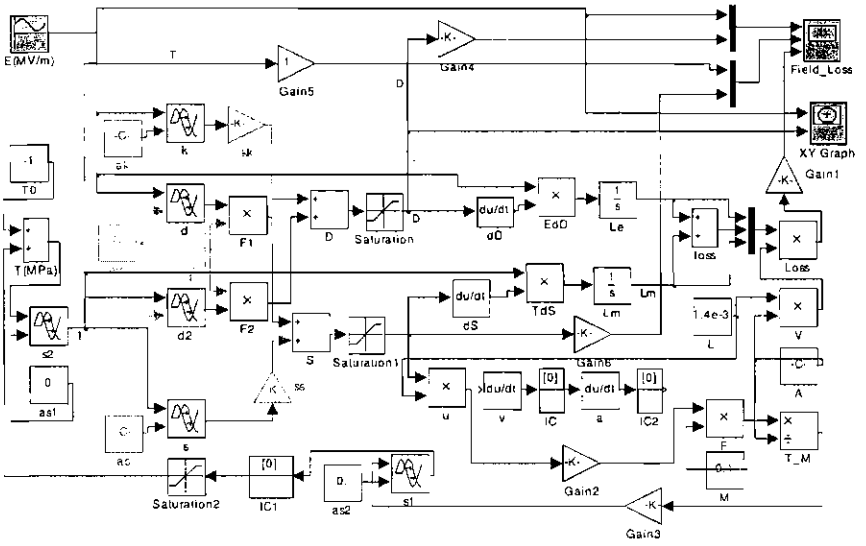

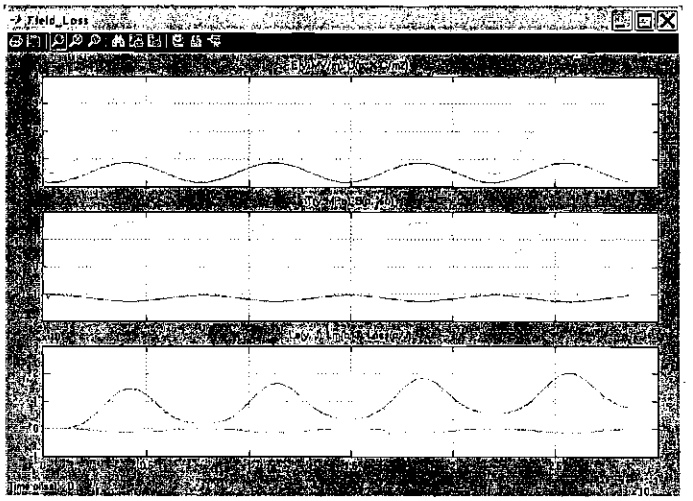

Figure 11. Simulink diagram and output.

4 Constitutive Modeling of Ferroelectric Material Loss

Instead of using complex coefficients, the hysteresis may be modeled by considering the changes of remnant electric displacement and remnant strain under electric field and stress. Change of the remnant electric displacement reflects domain reorientations and domain wall movements. Therefore it is directly connected to losses. In the following we will find the expression for the remnant electric displacement as a function of applied electric field and stress. We will start with the constitutive formulation of ferroelectrics.

4.1 Constitutive Formulation

More details of the constitutive behavior of ceramic ferroelectric materials are needed to take the next step in formulating constitutive laws. We desire phenomenological constitutive laws within a thermodynamics framework. For a linear reversible piezoelectric material one fixes the remanent terms and performs a Taylor series expansion to obtain constitutive laws. This gives the constants for mechanical and electrical compliance as well as the electro-mechanical coupling. In the case of the material that undergoes ferroelectric reorientation, several things happen. The single domain single crystal regions are linear piezoelectric within a certain range of loading. In this region the material is anisotropic in its elastic, piezoelectric, and dielectric properties. Outside of that range there can be field induced phase transformations.

Within a single crystal the boundaries between regions of like polarization (domain walls) find compatible orientations. This satisfies boundary conditions of strain and electric displacement compatibility and minimizes inter-domain stress and electric fields. At the grain scale, however, strain incompatibilities are reduced through non 180° domain walls within the grain. Similar statement for polarization incompatibilities.

The stress and electric field are related to the elastic terms. The linear piezoelectric constitutive behavior with fixed remanent strain and fixed remanent polarization is given by

$$\sigma = c\varepsilon^e - hD^e$$
$$E = -h\varepsilon^e + \beta D^e$$

If the remanent terms change in response to applied loads, what are the constitutive laws that govern small changes of stress and electric field in response to changes of the governing variables? These can be obtained by expressing the stress and electric field in terms of the independent variables and taking partial derivatives.

$$\sigma = \sigma\left(\varepsilon^e, D^e, \varepsilon^r, D^r, T\right)$$
$$E = E\left(\varepsilon^e, D^e, \varepsilon^r, D^r, T\right)$$

$$\Delta\sigma = \frac{\partial\sigma}{\partial\varepsilon^e}\Delta\varepsilon^e + \frac{\partial\sigma}{\partial D^e}\Delta D^e + \frac{\partial\sigma}{\partial\varepsilon^r}\Delta\varepsilon^r + \frac{\partial\sigma}{\partial D^r}\Delta D^r + \frac{1}{2}\left[\begin{array}{l} \frac{\partial^2\sigma}{\partial\varepsilon^{e2}}\Delta\varepsilon^e\Delta\varepsilon^e + 2\frac{\partial^2\sigma}{\partial\varepsilon^e\partial D^e}\Delta\varepsilon^e\Delta D^e + \\ 2\frac{\partial^2\sigma}{\partial\varepsilon^e\partial\varepsilon^r}\Delta\varepsilon^e\Delta\varepsilon^r + 2\frac{\partial^2\sigma}{\partial\varepsilon^e\partial D^r}\Delta\varepsilon^e\Delta D^r + \\ 2\frac{\partial^2\sigma}{\partial D^e\partial\varepsilon^r}\Delta D^e\Delta\varepsilon^r + 2\frac{\partial^2\sigma}{\partial D^e\partial D^r}\Delta D^e\Delta D^r \\ 2\frac{\partial^2\sigma}{\partial\varepsilon^r\partial D^r}\Delta\varepsilon^r\Delta D^r + \frac{\partial^2\sigma}{\partial D^{e2}}\Delta D^e\Delta D^e + \\ \frac{\partial^2\sigma}{\partial\varepsilon^r\partial\varepsilon^r}\Delta\varepsilon^r\Delta\varepsilon^r + \frac{\partial^2\sigma}{\partial D^r\partial D^r}\Delta D^r\Delta D^r \end{array}\right]$$

where the first order terms give

$$\frac{\partial\sigma}{\partial\varepsilon^e} = c,$$
$$\frac{\partial\sigma}{\partial\varepsilon^r} = \frac{\partial c}{\partial\varepsilon^r}\varepsilon^e - \frac{\partial h}{\partial\varepsilon^r}D^e$$
$$\frac{\partial\sigma}{\partial D^e} = -h$$
$$\frac{\partial\sigma}{\partial D^r} = \frac{\partial c}{\partial D^r}\varepsilon^e - \frac{\partial h}{\partial D^r}D^e$$

Combining the first four terms of the series expansion gives

$$\Delta\sigma = c\Delta\varepsilon^e + \left(\frac{\partial c}{\partial\varepsilon^r}\varepsilon^e - \frac{\partial h}{\partial\varepsilon^r}D^e\right)\Delta\varepsilon^r - h\Delta D^e + \left(\frac{\partial c}{\partial D^r}\varepsilon^e - \frac{\partial h}{\partial D^r}D^e\right)\Delta D^r$$

If we define out reference state such that the stress and electric field go to zero when the elastic components go to zero we can get rid of some of the deltas to arrive at

$$\sigma = c\varepsilon^e + \left(\frac{\partial c}{\partial \varepsilon^r}\varepsilon^e - \frac{\partial h}{\partial \varepsilon^r}D^e\right)\Delta\varepsilon^r - hD^e + \left(\frac{\partial c}{\partial D^r}\varepsilon^e - \frac{\partial h}{\partial D^r}D^e\right)\Delta D^r$$

which can be factored into

$$\sigma = \left(c + \frac{\partial c}{\partial \varepsilon^r}\Delta\varepsilon^r + \frac{\partial c}{\partial D^r}\Delta D^r\right)\varepsilon^e - \left(h + \frac{\partial h}{\partial \varepsilon^r}\Delta\varepsilon^r + \frac{\partial h}{\partial D^r}\Delta D^r\right)D^e$$

If we back track to the origination of the coupled constitutive law, it was obtained from a series expansion in which all of the terms were increments. Putting our result in that form gives

$$\dot{\sigma} = \left(c + \frac{\partial c}{\partial \varepsilon^r}\dot{\varepsilon}^r + \frac{\partial c}{\partial D^r}\dot{D}^r\right)\dot{\varepsilon}^e - \left(h + \frac{\partial h}{\partial \varepsilon^r}\dot{\varepsilon}^r + \frac{\partial h}{\partial D^r}\dot{D}^r\right)\dot{D}^e$$

and similarly

$$\dot{E} = -\left(h + \frac{\partial h}{\partial \varepsilon^r}\dot{\varepsilon}^r + \frac{\partial h}{\partial D^r}\dot{D}^r\right)\dot{\varepsilon}^e + \left(\beta + \frac{\partial \beta}{\partial \varepsilon^r}\dot{\varepsilon}^r + \frac{\partial \beta}{\partial D^r}\dot{D}^r\right)\dot{D}^e$$

These incremental laws govern the constitutive behavior and have the Maxwell symmetry.

We now need to develop the functions $c(\varepsilon^r), h(D^r), \kappa(D^r)$ as well as the equations governing the evolution of the remnant terms.

This can be done most readily using micromechanics and volume averaging. Micromechanical models in which the volume fraction of each variant evolves at a rate proportional to the driving force for that evolution will give rise to the functions we are seeking that govern minor hysteresis loops. We can also add in driving forces for phase transformations.

The second law states that the dissipation rate will be non-negative:

$$\sigma_{ji}\dot{\varepsilon}^r_{ij} + E_j\dot{D}^r_i \geq 0$$

4.2 Domain Engineering and Phase Transitions

The rhombohedral (R) phase has a spontaneous polarization in the <111> direction and the orthorhombic (O) phase has a spontaneous polarization in <110> direction. Crystal

variants present in a <110> poled single crystal and the rhombohedral-orthorhombic (R-O) phase transition under electric field E_3 and stress σ_{22} are illustrated in Figure 12. Electric field induced rhombohedral to orthorhombic phase change has been observed in <110> oriented PMN-30%PT (Viehland et al., 2002; Feng et al. 2003) and PZN-4.5%PT(Liu and Lynch, 2003).

Figure 13 is a schematic of a crystal variant representation of the average domain structure and possible phase transitions driven by electric field and stress loading in the <001> direction. An electric field induced phase transition between the rhombohedral and tetragonal (R-T) phases has been observed (Liu et al., 1999; Ren, Liu and Mukherjee, 2002; Noheda et al., 2001; Viehland, 2000; Park and Hackenberger, 2002; Chen, Zhang and Luo, 2002).

The phase stability of the relaxor single crystals depends on the electrical, mechanical and thermal conditions. Changes of temperature, electric field and stress lead to polarization switching and phase transitions in these crystals and hence dramatically alter their electromechanical properties.

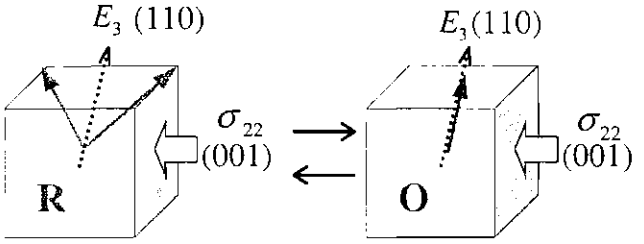

Figure 12. Crystal variants in <110> poled (32-mode) single crystals

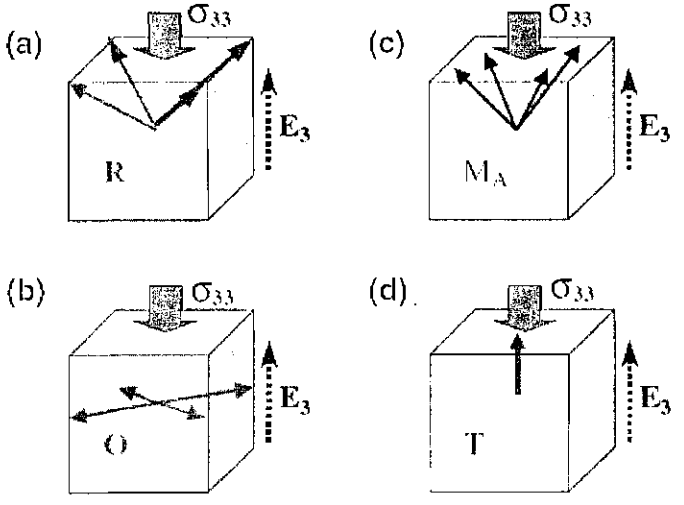

Figure 13. Crystal variants in <001> poled (33-mode) single crystals

4.3 Polarization Switching Model

When an opposite electric field reach certain level (the coercive field Ec), polarization switching (effectively 180°) occurs. When a compressive stress in the poling direction reached certain level (the coercive stress Tc), depolarization (effectively 90° switching) occurs. Combination of the electric field and the stress determines the poling (switching) or depoling process.

For the 33-mode, a compressive stress in the poling direction acts against an electric field in the poling direction, while it works together with an opposite electric field during the depoling stage. When E/Ec > T/Tc, we consider this as a polarization switching (effectively 180°) process. The normalized driving force for poling is expressed as:

$$ET = \frac{E}{Ec} - \frac{T}{Tc}$$

When E/Ec < T/Tc, we consider this as a depolarization (effectively 90° switching) process. The normalized driving force for depoling is expressed as:

$$ET = \frac{E}{Ec} + \frac{T}{Tc}$$

The switching/depoling criterion is ET >= 1. Hyperbolic tangent functions are used to simulate the poling and depoling process. Below shows the simulated D^r-E curves at T_0 = 0, Tc, 2Tc. At zero stress, no depolarization occurs therefore a smooth curve is obtained. When there is a compressive stress applied, there is a depoling stage before the reverse polarization. A better function for the depolarization process is needed to model a smooth depoling-repoling process and the minor depolarization during electric field unloading. Rate dependence may be included by introducing phase angles into the model. The phase angles may be field and temperature dependent.

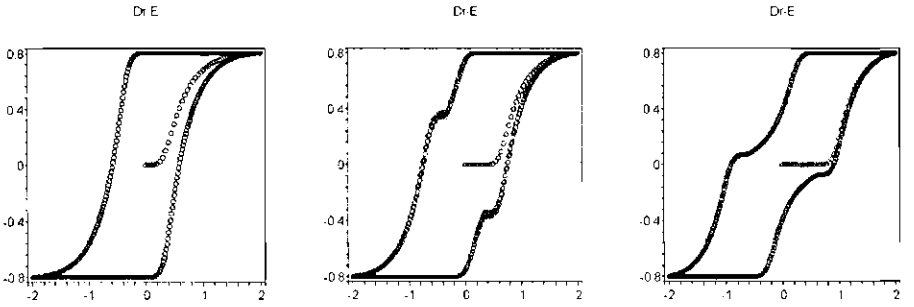

$T_0 = 0$, $T_0 = Tc$, $T_0 = 2Tc$

Figure 14. Dr-E curves at different stress preloads

4.4 Depolarization Model

Here remnant electric displacement as a function of stress and electric field is modeled. The effect of stress (preload, T0) may be modeled by the following function:

For 33-mode (depoling):

$$Dr1 = Dr0 - \frac{Dr0\left(\tanh\left(\frac{T0 - Tc}{Tc}\right) + \tanh(1)\right)}{1 + \tanh(1)} \qquad \text{(Dr0~0)}$$

For 32-mode (polarization strengthening):

$$Dr1 = Dr0 + (1 - Dr0)\tanh\left(\frac{T0}{Tc}\right) \qquad \text{(Dr0~1)}$$

The effect of electric field (polarization strengthening) is modeled with:

$$Dr = Dr1 + (1 - Dr1)\tanh\left(\frac{E}{Ec}\right) \qquad \text{(Dr1~1)}$$

Change of D^r during the electric field cycling is then:

$$\delta Dr = (1 - Dr1)\left(\tanh\left(\frac{E0 + Ea}{Ec}\right) - \tanh\left(\frac{E0 - Ea}{Ec}\right)\right)$$

Remnant electric displacement versus electric field at different stress preloads and change of remnant electric displacement versus electric field amplitude (zero bias) at different stress preloads are plotted as follows. The opposite effects of the stress in the two modes are apparent.

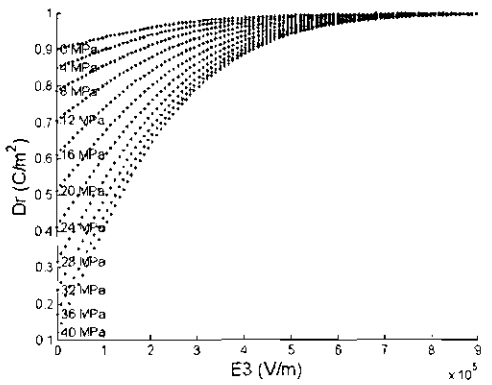

(a) Dr, 33-mode

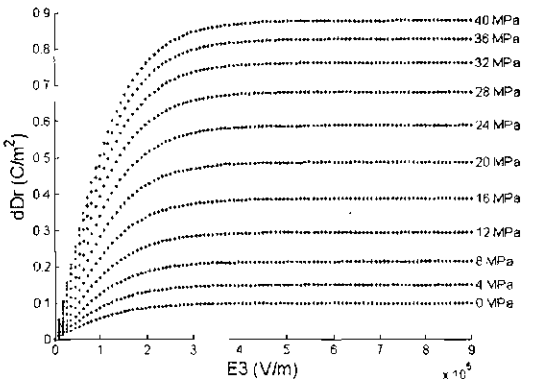

(b) ΔDr, 33-mode

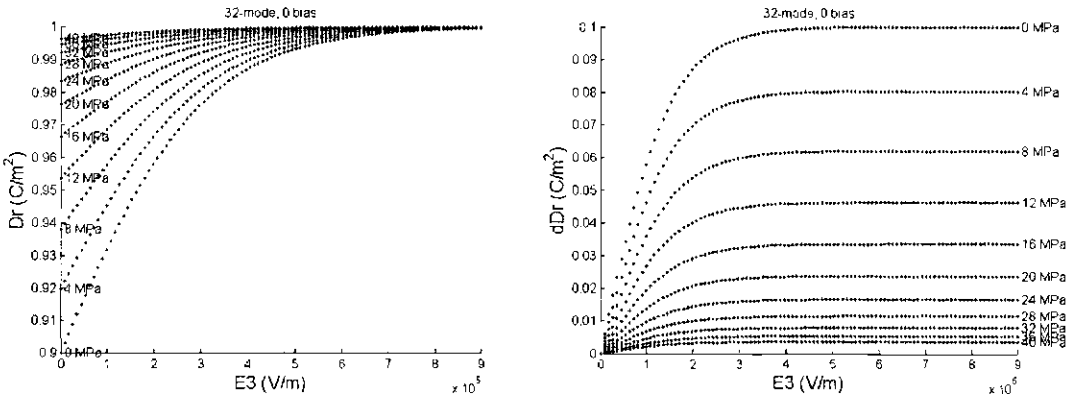

(c) Dr, 32-mode (d) ΔDr, 32-mode

Figure 15. Remnant electric displacement as a function of stress and electric field

These functions for depolarization may be adapted into the switching model.

To introduce the hysteresis, we need to set up a relation between loss and ΔDr. We may assume the dielectric loss tangent to be proportional to ΔDr.

Note that the previous models do not capture phase transitions that may occur in both 33-mode and 32-mode rhombohedral single crystals.

4.5 Model for Switching and Phase Transformations

A model is constructed to capture both polarization switching and phase transformation. The remnant electric displacement D^r is expressed as a function of electric field and stress:

$$Dr := D0 + (Dr1 - D0)\tanh\left(\frac{k\,E1}{Ec}\right) + \frac{E2\,(Dr2 - Dr1)\left(1 + \tanh\left(\frac{kph\,(|E2| - Ec2)}{Ec}\right)\right)}{2\,(|E2| + 1\,10^{-20})}$$

There are three terms in this function. The first term D0 is a function of stress T as well as electric field bias E0 and amplitude Ea:

$$D0 := Dr1\,\tanh\left(\frac{kD0\,E0}{Ea}\right) DrT$$

$$DrT := 1 - \frac{\left(1 - \tanh\left(\frac{0.5\,Tc}{T0}\right)\right)\left(\tanh\left(\frac{taoT\,(T0 - Tc)}{Tc}\right) + \tanh(taoT)\right)}{1 + \tanh(taoT)}$$

Tc is the coercive stress and $kD0$ and $taoT$ are two parameters. DrT is plotted as follows.

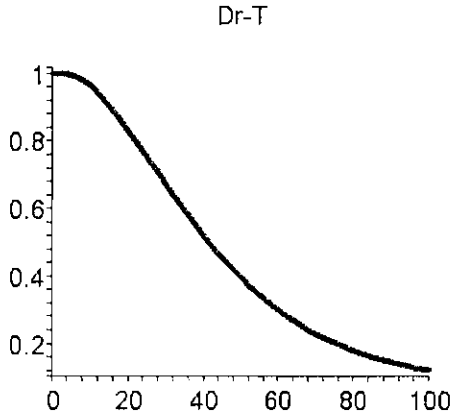

Figure 16. Depolaization under stress

The second term of Dr represents the polarization switching process. In this term *E1* is the electric field with a delay of aD:

$$E1 := E0 + Ea \sin(2 \pi w t - aD)$$

k is a parameter

$$k := \frac{\operatorname{arctanh}\left(\frac{Dr0}{Dr1}\right) Ec}{Ea \sin(aD)} \qquad aD := 1.001 \arcsin\left(\frac{Ec}{Ea}\right)$$

The third term of Dr represents the phase transformation process. In this term *E2* is the electric field with a delay of aD2:

$$E2 := E0 + Ea \sin(2 \pi w t - aD2)$$

Ec2 is the electric field level at which the phase transition occurs.

$$Ec2 := 1.4 + \frac{T0\ Ec}{Tc}$$

kph is a parameter.

The Dr-E curve under unipolar electric field cycling is shown below. At zero stress preload, the curve has two hysteresis loops and two flat regions. The hysteresis at low electric field is due to depoling. This is more severe as the stress preload increases. Above certain electric field level, the polarization of the <001> rhombohedral phase single crystal is stabilized (the first flat region). As the electric field further increases, a rhombohedral to monoclinic phase transformation is induced, resulting in the second hysteresis loop. After the phase transformation, the crystal is again stabilized in the monoclinic phase. The stress preload leads to higher phase transition field level.

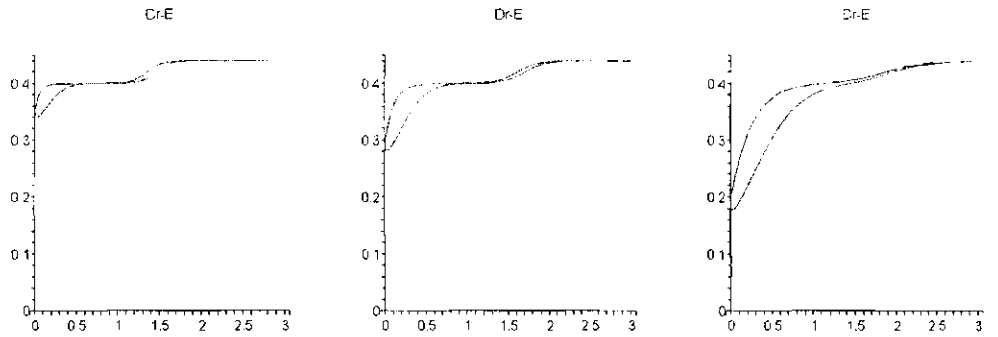

Figure 17. Depolarization and phase change under unipolar electric field with stress preload (a) T_0 = 0, (b) Tc, (c) 2Tc.

This model is able to simulate the polarization switching process as well. Shown below are the simulations or D^r-E and S^r-E curves under bipolar electric field cycling at stress preload T_0 = 0, Tc, 2Tc. Here the remnant strain is computed from the remnant electric displacement through electrostrictive relations. It is shown that the major hysteresis loop due to polarization switching and the minor hysteresis loops due to phase transition are predicted with a smooth function. The stress preload leads to depolarization and change of the D^r-E and S^r-E curves. The coercive field and remnant electric displacement as parameters are put in the model. Further development is needed to capture the stress cycling behavior.

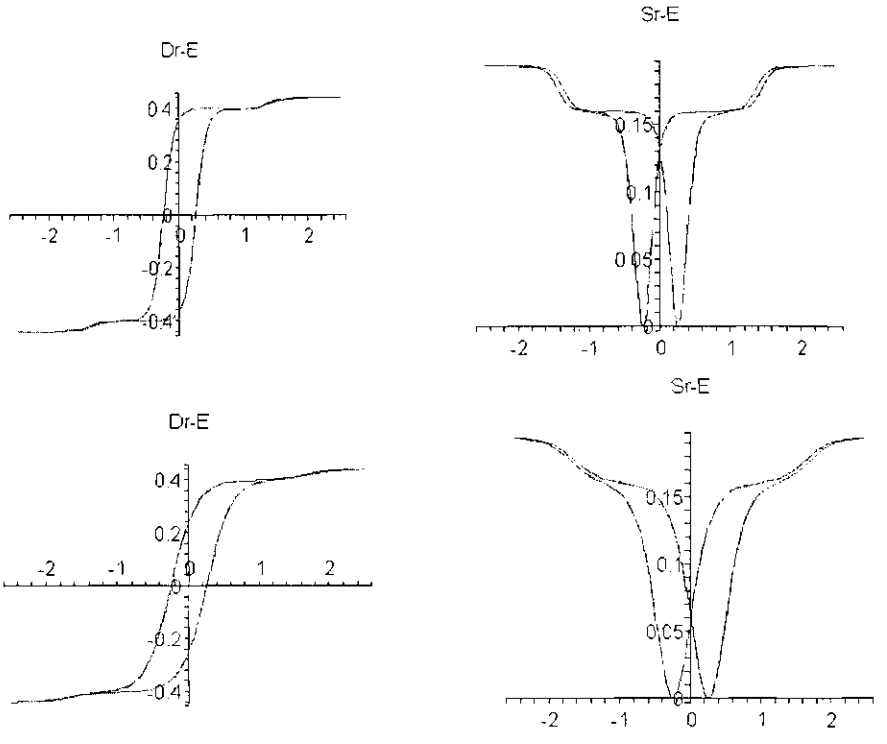

T_0 = 0

T_0 = Tc

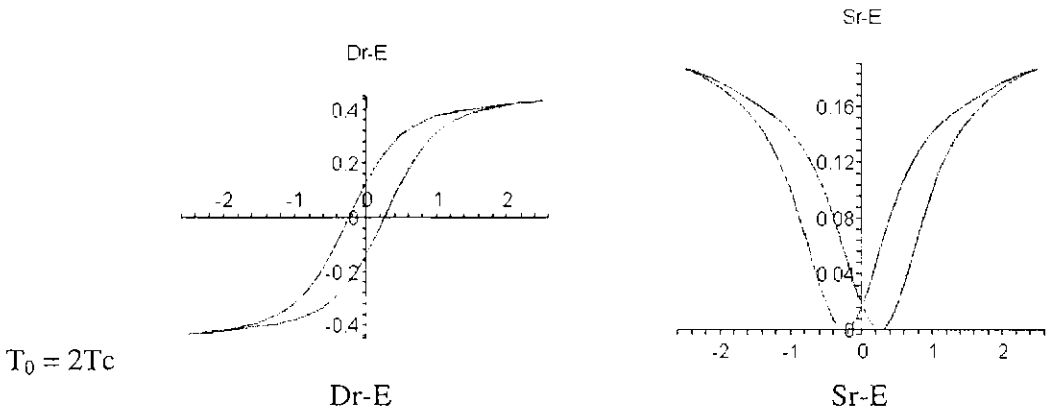

Figure 18. Simulations of D^r-E and S^r-E curves

With the D^r and S^r data, the losses in a cycle can be computed by integration. Effective loss modulus and loss tangents can also be computed from the losses.

5 Temperature Increase due to Heat Generation

Assume the irreversible work (electrical loss and mechanical loss) are all converted into heat. The temperature increase of the transducer can then be computed:

$$\Delta T = \frac{efv_e}{kA}$$ (Pritchard 2004)

Here e is the total loss in an electric field cycle (J/mm^3/cycle), f is the field frequency, v_e is the effective volume of the piezoelectric element, k is the overall heat transfer coefficient and A the surface area of the transducer.

Based on the depolarization model, temperature profile of a 33-mode actuator under different electric field biases, amplitudes, frequencies and different stress preloads are simulated and plotted in the following. At low frequency, induced stress is small therefore heat generation is mainly due to dielectric loss. Note that the simulations here do not mean to be accurate. The actual loss at different loading conditions and the heat transfer coefficient will be needed in order to predict the temperature increase.

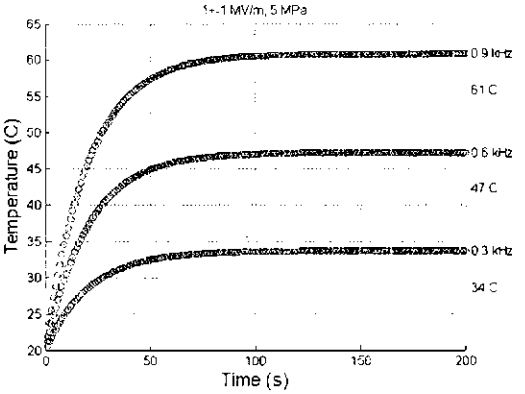

(a) At different frequencies

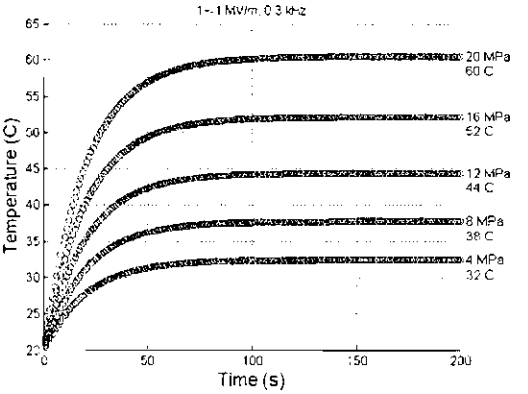

(b) At different stress preloads

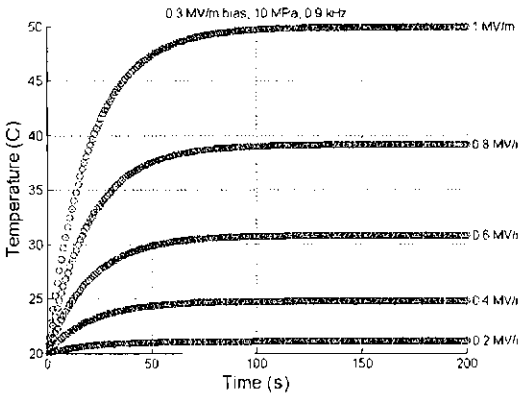

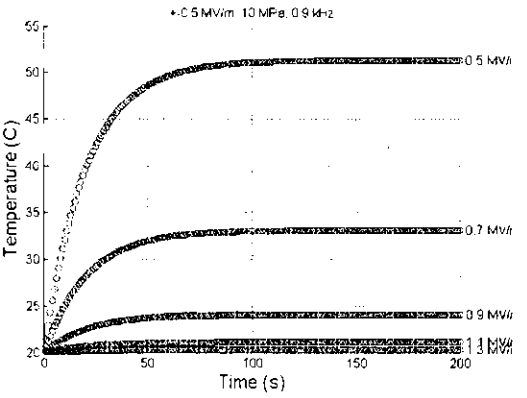

(c) With different electric field amplitudes (d) At different electric field biases

Figure 19. Temperature profile of the actuator under different electric field biases, amplitudes, frequencies and different stress preloads.

Figure 20 plots the field amplitude to achieve u=1 μm displacement and the corresponding temperature increase. When the electric field frequency approaches the resonant frequency, the required electric field amplitude is reduced, at the same time large stress is induced associated with large mechanical loss.

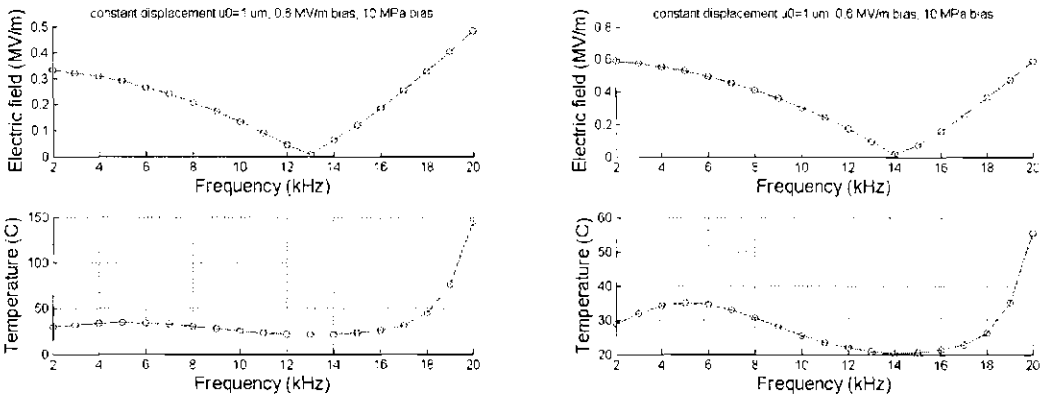

(a) 33-mode (b) 32-mode

Figure 20. Field strength and temperature increases to achieve u = 1 μm displacement at different frequency.

6 Summary

The losses and heat generation of a transducer has been modeled. There are two levels in the modeling efforts: transducer system level and material level. Applied electric field and bias, stress preload, frequency and dynamic response of the transducer has been considered.

At the transducer system level, the dynamics of a transducer structure was analyzed. The linear vibration problem was first solved and the electric field E induced displacement u and stress as functions of frequency were obtained. Loss tangents were then used to compute dielectric and mechanical loss. Losses in a field cycle were compute by path integration. The temperature increase profile of the transducer was computed with input of total losses and overall heat transfer coefficient.

At the material level, loss mechanism and hysteretic material models were investigated. For complex electromechanical loadings, the complex coefficients are not sufficient to capture the complex polarization switching and phase transition features of ferroelectric single crystals. The dielectric and mechanical losses can be computed as the irreversible work done by the electric field and stress. Constitutive models were developed to predict

the evolution of remnant electric displacement and remnant strain as functions of electric field, Stress, frequency and temperature.

The response of a transducer will depend on the nonlinear and hysteretic behavior of the piezoelectric material. Additional efforts are needed to finish the remnant electric displacement based hysteresis model for combined electromechanical loadings. Experimental data and the model will then be implemented for the dynamics system of transducers. Developed computer codes will be further debugged and packed with proper user interface and documentation.

Appendix

A. Thermodynamics of Electromechanical Coupling Materials

Work and Energy

Mechanical work rate: The mechanical work rate is given by the integration of tractions over displacements

$$\dot{W}^m = \int_{\partial\Gamma} t_i \dot{u}_i dS$$

Electrical work rate: The electrical work rate is given by

$$\dot{W}^e = \int \phi \dot{\omega} dS$$

The rate of change of kinetic energy of the body is given by

$$\dot{K} = \frac{d}{dt} \int_{\Gamma} \frac{1}{2} \rho v_j v_j dV$$

The rate of change of internal energy is given by

$$\dot{E} = \frac{d}{dt} \int_{\Gamma} \rho e dV$$

and the rate heat is being added to the body is given by

$$\dot{Q} = \int_{\Gamma} \dot{r} dV - \int_{\partial\Gamma} \dot{q}_i n_i dS$$

where $\dot{r}$ is the rate at which heat is generated within the volume from an external source such as microwaves (to be distinguished from heat generated by a dissipative process

driven by a mechanical or electrical source; it is very important to recognize that $\dot{r}$ does not include heat generated through dissipative processes such as stress driven domain wall motion), and $\dot{q}_i$ are components of the outward heat flux vector and thus the minus sign to obtain the inward heat flux. Note the dot over the *Q, r, and q* indicates that these are rates. This dot is usually omitted in the literature.

Equation of Energy Balance

The expression for energy balance is

$$\dot{W}^m + \dot{W}^e + \dot{Q} = \dot{K} + \dot{E}$$

where each of the terms on the LHS represent work done on the body and of heat added to the body, i.e. a sum of all energy transferred to the body; and the terms on the RHS represent where this energy went.

Combining these expressions gives

$$\int_{\partial\Gamma} t_i \dot{u}_i dS + \int_{\partial\Gamma} \phi \dot{\alpha} dS + \int_{\Gamma} \dot{r} dV - \int_{\partial\Gamma} \dot{q}_i n_i dS = \frac{d}{dt} \int_{\Gamma} \frac{1}{2} \rho v_j v_j dV + \frac{d}{dt} \int_{\Gamma} \rho \dot{e} dV$$

The surface integrals on the LHS can be written as volume integrals

$$\int_{\partial\Gamma} \sigma_{ji} n_j \dot{u}_i dV - \int_{\partial\Gamma} \phi \dot{D}_j n_j dV + \int_{\Gamma} \dot{r} dV - \int_{\partial\Gamma} \dot{q}_i n_i dS = \frac{d}{dt} \int_{\Gamma} \frac{1}{2} \rho v_j v_j dV + \frac{d}{dt} \int_{\Gamma} \rho \dot{e} dV$$

which becomes

$$\int_{\Gamma} \left(\sigma_{ji} \dot{u}_i\right)_{,j} dV - \int_{\Gamma} \left(\phi \dot{D}_j\right)_{,j} dV + \int_{\Gamma} \dot{r} dV - \int_{\Gamma} \dot{q}_{j,j} dV = \frac{d}{dt} \int_{\Gamma} \frac{1}{2} \rho \dot{u}_j \dot{u}_j dV + \frac{d}{dt} \int_{\Gamma} \rho \dot{e} dV$$

Mechanical equilibrium is expressed as

$$\sigma_{ji,j} + f_i = \rho \ddot{u}_i$$

and quasi-static charge equilibrium is expressed by

$$D_{j,j} = \rho_v$$

The integrals thus become

$$\int_\Gamma (\sigma_{ji}\dot{u}_i)_{,j}\,dV = \int_\Gamma (\sigma_{ji,j}\dot{u}_i + \sigma_{ji}\dot{u}_{i,j})dV = \int_\Gamma ((\rho\ddot{u}_i - f_i)\dot{u}_i + \sigma_{ji}\dot{u}_{i,j})dV = \int_\Gamma ((\rho\ddot{u}_i - f_i)\dot{u}_i + \sigma_{ji}\dot{\varepsilon}_{ij})dV$$

and

$$-\int_\Gamma (\phi\dot{D}_j)_{,j}\,dV = -\int_\Gamma (\phi_{,j}\dot{D}_j + \phi\dot{D}_{j,j})dV = \int_\Gamma (E_j\dot{D}_j - \phi\dot{\rho}_v)dV$$

For a homogeneous medium the kinetic energy term becomes

$$\frac{d}{dt}\int_\Gamma \frac{1}{2}\rho\dot{u}_j\dot{u}_j dV = \int_\Gamma \rho\dot{u}_j\ddot{u}_j dV$$

Upon substitution one obtains

$$\int_\Gamma ((\rho\ddot{u}_i - f_i)\dot{u}_i + \sigma_{ji}\dot{\varepsilon}_{ij})dV + \int_\Gamma (E_j\dot{D}_j - \phi\dot{\rho}_v)dV + \int_\Gamma \dot{r}dV - \int_\Gamma \dot{q}_{j,j}dV = \int_\Gamma \rho\dot{u}_j\ddot{u}_j dV + \frac{d}{dt}\int_\Gamma \rho\dot{e}dV$$

which can be rearranged to give the *general equation of energy balance*

$$\int_\Gamma (-f_i\dot{u}_i + \sigma_{ji}\dot{\varepsilon}_{ij})dV + \int_\Gamma (E_j\dot{D}_j - \phi\dot{\rho}_v)dV + \int_\Gamma \dot{r}dV - \int_\Gamma \dot{q}_{j,j}dV = \int_\Gamma \rho\dot{e}dV$$

In the absence of body forces and motion of body charges we obtain

$$\int_\Gamma (\sigma_{ji}\dot{\varepsilon}_{ij})dV + \int_\Gamma (E_j\dot{D}_j)dV + \int_\Gamma (\dot{r} - \dot{q}_{j,j})dV = \int_\Gamma \rho\dot{e}dV$$

Note that the motion of body charges is a source of dissipation and will contribute to minor hysteresis loops. This is an electrical conductivity term that will be neglected relative to effects of domain wall motion.

The volume may now be shrunk to a point to obtain a local expression for the rate of change of internal energy.

$$\rho\dot{e} = \sigma_{ji}\dot{\varepsilon}_{ij} + E_j\dot{D}_j + \dot{r} - \dot{q}_{j,j}$$

This expression is valid even if the strain and electric displacement increments contain irreversible (dissipative) terms.

Second Law of Thermodynamics

At this point, temperature and entropy are introduces as work conjugate variables. Thermodynamic processes progress such that the dissipation is always positive or zero.

This means that the increase of thermal energy of the body is always greater than the heat added.

$$T\dot{S} \geq \dot{Q}$$

where

$$\dot{S} = \int_{\Gamma} \rho \dot{s} dV$$

thus

$$T\dot{S} = \int_{\Gamma} \rho T \dot{s} dV \geq \int_{\Gamma} (\dot{r} - \dot{q}_{i,i}) dV$$

or locally,

$$\rho T \dot{s} \geq (\dot{r} - \dot{q}_{i,i})$$

Irreversible Strain and Electric Displacement Components

To address irreversible strain and irreversible electric displacement the material structure must be considered. To do this, a volume is considered that is sufficiently small that the average stress, strain, electric displacement, and electric field can be considered uniform; yet it must be sufficiently large that details of the microstructure can be replaced with volume average behavior. This raises the issue of energy stored at the micro-structural length scale associated with incompatible strain and electric displacement components. The incompatibilities become compatible through reversible deformation accompanied by local stress and local electric field. The result is that energy can be stored in the microstructure. The macroscopic observable variables are the total strain, the elastic strain, the remnant strain, the total electric displacement, the reversible electric displacement, the remnant electric displacement, and the temperature. The micro-structurally stored energy gives rise to phenomena such as logarithmic aging of the piezoelectric coefficients, relaxation of the remnant strain with time, etc.

At this point the concept of internal variables is introduced. The directly measurable variables are the total strain, the total electric displacement, the tractions applied to the surface, and the charges on the surface. One can also measure the electric potential and the temperature. The independent variables associated with external work done on the body are the strain and electric displacement. If the body is electro-mechanically loaded from zero and subsequently unloaded to zero, the macroscopic reversible strain and reversible polarization are zero. Permanent changes in strain and polarization are observed. These are the remnant strain and remnant polarization.

The macroscopic strain rate and electric displacement rate are partitioned into reversible and irreversible components. These are expressed as

$$\dot{\varepsilon}_{ij} = \dot{\varepsilon}^e_{ij} + \dot{\varepsilon}^r_{ij}$$

$$\dot{D}_i = \dot{D}^e_i + \dot{D}^r_i$$

In addition, there is reversible strain and polarization at the micro-structural level that give rise to local stress and local electric field. Although the volume averages of these local fields are zero, the stored energy associated with these quantities is non-zero. These must be included in the expression for the energy.

The partitioned strain and electric displacement can be substituted into the expression for internal energy to obtain

$$\rho\dot{e} = \sigma_{ji}\left(\dot{\varepsilon}^e_{ij} + \dot{\varepsilon}^r_{ij}\right) + E_j\left(\dot{D}^e_i + \dot{D}^r_i\right) + \dot{r} - \dot{q}_{j,j}$$

Micro-structural Fields

This is a local expression in which local fields are to be considered. If the volume element considered is large enough that there has been some homogenization of the local fields, a term must be included to account for the electrical and mechanical energy stored in the local fields for which the volume average terms (stress, strain, electric field, electric displacement) are zero. This will be brought in through the concept of the microstructural stress, microstructural strain, microstrutural electric field, and microstructural electric displacement. The energy expression then becomes

$$\rho\dot{e} = \sigma_{ji}\dot{\varepsilon}^e_{ij} + E_j\dot{D}^e_i + \sigma_{ji}\dot{\varepsilon}^r_{ij} + E_j\dot{D}^r_i + \sigma^\mu_{ij}\dot{\varepsilon}^\mu_{ij} + E^\mu_i\dot{D}^\mu_i + \dot{r} - \dot{q}_{j,j}$$

The microstrutural terms are related through a constitutive law and have magnitudes such that they give the correct contribution to the internal energy. The microstructural stress and electric fields contribute to the driving forces for domain wall motion (evolution of the remanent strain and remanent polarization). This accounts for the driving force for creep and aging behavior. An example of where these microstructural terms arise is intergranular stress associated with poling a ferroelectric ceramic. Each grain can only be poled in certain crystallographic directions. It elongates in the polar direction and contracts in a plane perpendicular to the polar direction. The grains are bound together at their boundaries. Due to their different spatial orientations they are constrained at their boundaries. A hypothetical fully poled ceramic (sufficient large field to give single domain grains) would thus have a large elastic stress within each grain. Some grains would be in tension and some in compression, depending on their orientation. The volume average stress would be zero, but the strain energy associated with the microstructural stress would not be zero. This microstructural stress would drive the nucleation and motion of domain walls such that the domains would reduce the microstructural energy. The application of an external field can thus move domain walls in one direction and on removal of the field the intergranular stress can move them back. The dissipation associated with this process gives rise to minor hysteresis loops. The same arguments apply to local electric energy. If there are space charges within a crystal,

domain structures will form that minimize the energy of the structure. This will give rise to domain walls that satisfy the electrical term $D_{j,j} = \rho_v$. The domain walls will thus be compatible with the local charge distribution. If the applied stress or electric field forces domain wall motion away from the charge, a local field will be generated that attracts the domain wall back to the charge. If the charge can diffuse in the structure, it will follow the domain wall motion if the domain wall moves slowly enough.

Dissipation

The remanent strain and remanent electric displacement increments are dissipative. The dissipation is associated with domain wall motion and may include effects associated with diffusion of charge as domain walls move away from local charges. The heat added plus the dissipation shows up in the thermal term.

$$\rho\dot{e} = \sigma_{ji}\dot{\varepsilon}^{e}_{ij} + E_j\dot{D}^{e}_{i} + \sigma^{\mu}_{ij}\dot{\varepsilon}^{\mu}_{ij} + E^{\mu}_{i}\dot{D}^{\mu}_{i} + \rho T\dot{s}$$

where

$$\rho T\dot{s} = \sigma_{ji}\dot{\varepsilon}^{r}_{ij} + E_j\dot{D}^{r}_{i} + \dot{r} - \dot{q}_{j,j}$$

This suggests partitioning the entropy into that portion generated by internal dissipative processes, and changes in entropy associated with heat added from the surroundings, leading to

$$\rho T\left(\dot{s}^{d} + \dot{s}^{q}\right) = \sigma_{ji}\dot{\varepsilon}^{r}_{ij} + E_j\dot{D}^{r}_{i} + \dot{r} - \dot{q}_{j,j}$$

where

$$\rho T\dot{s}^{d} = \sigma_{ji}\dot{\varepsilon}^{r}_{ij} + E_j\dot{D}^{r}_{i}$$

and

$$\rho T\dot{s}^{q} = \dot{r} - \dot{q}_{j,j}$$

There is also an entropy term associated with reversible constitutive behavior that is important in the field coupled material. This term is associated with thermal expansion, pyroelectricity, and heat capacity.

This expression makes the direct connection between the dissipative increments of the strain and electric displacement and the generation of thermal energy. The second law states that these dissipative increments are always positive or zero (no negative dissipation) and that the result of dissipation is always an increase of thermal energy.

B. Complex Dielectric Constant and Dielectric Loss

Consider electric field
$E = E_a Cos(\omega t)$

And the induced electric displacement
$D = D_a Cos(\omega t - \delta)$

The work done by the electric field is

$dw_e = EdD = E_a Cos(\omega t)\, d(D_a Cos(\omega t - \delta)) = -\omega E_a D_a Cos(\omega t)\, Sin(\omega t - \delta) dt$

Dielectric loss energy during an electric field cycle per unit volume of the dielectrics can be computed by integration:

$$L_e = \oint EdD = \int_0^{2\pi/\omega} E(dD/dt)dt = \pi E_a D_a Sin\delta = \pi \varepsilon'' E_a^2 = \pi \varepsilon' E_a^2 \tan\delta$$

Another expression:

Electric field $E = \frac{1}{2}(E^* + \bar{E}^*)$:

$$E := \frac{1}{2} Ea \left(e^{(I \omega t)} + e^{(-I \omega t)}\right)$$

Electric displacement

$$Dele := \frac{1}{2} Da \left(e^{(I (\omega t - \delta))} + e^{(-I (\omega t - \delta))}\right)$$

$$dD := \frac{1}{2} I Da \omega \left(e^{(I (\omega t - \delta))} - e^{(-I (\omega t - \delta))}\right)$$

$dw_e = EdD$:

$$dw := t \to \frac{1}{4} I Ea \left(e^{(I \omega t)} + e^{(-I \omega t)}\right) Da \omega \left(e^{(I (\omega t - \delta))} - e^{(-I (\omega t - \delta))}\right)$$

It can be simplified as

$$\frac{1}{4} I Ea Da \omega \left(\frac{\left(e^{(I \omega t)}\right)^2}{e^{(I \delta)}} - e^{(I \delta)} + \frac{1}{e^{(I \delta)}} - \frac{e^{(I \delta)}}{\left(e^{(I \omega t)}\right)^2} \right)$$

or

$$dw := \frac{1}{2} Ea\ Da\ \omega\ (\sin(\delta) - \sin(-\delta + 2\ \omega\ t))$$

Dielectric loss in a cycle $L_e = \oint EdD = \int_0^{2\pi/\omega} E(dD/dt)dt$:

$$Le := Ea\ Da \sin(\delta)\ \pi$$

Introduce $\varepsilon^* = \varepsilon' - I\ \varepsilon''$:

$$\varepsilon 1 - I\ \varepsilon 2 = \frac{Da\ e^{(-I\ \delta)}}{Ea}$$

$$\varepsilon 1 - I\ \varepsilon 2 = \frac{Da \cos(\delta)}{Ea} - \frac{I\ Da \sin(\delta)}{Ea}$$

$$\left\{ \varepsilon 2 = \frac{\varepsilon 1 \sin(\delta)}{\cos(\delta)},\ Da = \frac{\varepsilon 1\ Ea}{\cos(\delta)} \right\}$$

$$Le := Ea^2\ \varepsilon 1\ \pi \tan(\delta)$$

Reference

D. Damjanovic, in *Proceedings of the 4th International Conference on Electronic Ceramics and Applications, Sept. 5–7, 1994*, edited by R. Waser, S. Hoffmann, D. Bonnenberg, and Ch. Hoffmann (Augustinus, Aachen, Germany, 1994), Vol. 1, p. 239.

D. Damjanovic, M. Demartin, H. S. Shulman, M. Testorf, and N. Setter, Sens. Actuators A **53**, 353 (1996).

K. H. Hardtl, "Electrical and Mechanical Losses in Ferroelectric Ceramics,"Ceram. Int., 8 [4] 121–7 (1982).

M. L. James, G. M. Smith, J. C. Wolford, P. W. Whaley Vibration of Mechanical and Structural Systems: With Microcomputer Applications (Hardcover), Harper & Row, Publishers, Inc. New York, 1989.

K. UCHINO, "Piezoelectric Actuators and Ultrasonic Motors", (Kluwer Academic Publ., Boston, 1997)

Viehland, D. & Li, J. F. Anhysteretic field-induced rhombhohedral to orthorhombic transformation in <110>-oriented $0.7Pb(Mg_{1/3}Nb_{2/3})O_3$– $0.3PbTiO_3$ crystals. *J. Appl. Phys.* **92,** 7690–7692 (2002).

Feng, Z., Luo, H., Guo, Y., He, T. & Xu, H. Dependence of high electric-field-induced strain on the composition and orientation of $Pb(Mg_{1/3}Nb_{2/3})O_3$–$PbTiO_3$ crystals. *Solid State Commun.* **126,** 347–351 (2003).

Chen, K.-P., Zhang, X.-W., and Luo, H.-S. 2002. "Electric-field-induced phase transition of <001> oriented $Pb(Mg_{1/3}Nb_{2/3})O_3$–$PbTiO_3$ single crystals," *J. Phys. : Condens. Matter*, 14: 571-576.
Liu, S.F., Park, S.E., Shrout, T.R., and Cross, L.E. 1999. "Electric field dependence of piezoelectric properties for rhombohedral 0.955 $Pb(Zn_{1/3}Nb_{2/3})O_3$–0.045$PbTiO_3$ single crystals," *J. Appl. Phys.*, 85(5): 2810.
Noheda, B., Cox, D.E., Shirane, G., Guo, R., Jones, B., and Cross, L.E. 2001. "Stability of the monoclinic phase in the ferroelectric perovskite $PbZr_{1-x}Ti_xO_3$," *Phys. Rev. B*, 63(014103): 1-6.
Park, S.E.E. and Hackenberger, W. 2002. "High performance single crystal piezoelectrics: applications and issues," *Curr. Opin. Solid State Mater. Sci.*, 6(1): 11-18.
Ren, W., Liu, S.F., and Mukherjee, B.K. 2002. "Piezoelectric properties and phase transitions of [Left Angle Bracket] 001 [Right Angle Bracket] -oriented $Pb(Zn_{1/3}Nb_{2/3})O_3$–$PbTiO_3$ single crystals," *Appl. Phys. Lett.*, 80(17): 3174.
Viehland, D. 2000. "Symmetry-adaptive ferroelectric mesostates in oriented $Pb(BI_{1/3}BII_{2/3})O_3$–$PbTiO_3$ crystals," *J. Appl. Phys.*, 88(8): 4794-4806.
Damjanovic, D., 1997. Stress and frequency dependence of the direct piezoelectric effect in ferroelectric ceramics. Journal of Applied Physics 82, 1788.
Damjanovic, D., Demartin, M., 1996. Rayleigh law in piezoelectric ceramics. Journal of Physics D: Applied Physics 29, 2057.
Damjanovic, D., Demartin, M., 1997. Contribution of the irreversible displacement of domain walls to the piezoelectric effect in barium titanate and lead zirconate titanate ceramics. Journal of Physics: Condensed Matter 9, 4943.
Eitel, R.E., Shrout, T.R., Randall, C.A., 2006. Nonlinear contributions to the dielectric permittivity and converse piezoelectric coefficient in piezoelectric ceramics. Journal of Applied Physics 99, 124110.
Hall, D.A., 2001. Nonlinearity in piezoelectric ceramics. Journal of Materials Science 36, 4575.
Liu, T., Lynch, C.S., 2003. Ferroelectric properties of [110], [001] and [111] poled relaxor single crystals: measurements and modeling. Acta Materialia 51, 407-416.
Taylor, D.V., Damjanovic, D., 1997. Evidence of domain wall contribution to the dielectric permittivity in PZT thin films at sub-switching fields. Journal of Applied Physics 82, 1973.
Taylor, D.V., Damjanovic, D., 1998. Domain wall pinning contribution to the nonlinear dielectric permittivity in Pb(Zr, Ti)O₃ thin films. Applied Physics Letters 73, 2045.
Uchino, K., Hirose, S., 2001. Loss mechanisms in piezoelectrics: how to measure different losses separately. IEEE Transactions on Ultrasonics, Ferroelectrics and Frequency Control 48, 307.
Uchino, K., Zheng, J., Chen, Y.H., Du, X., Hirose, S., Takahashi, S., 2000. Loss mechanisms in piezoelectrics - extrinsic and intrinsic losses. Materials Research Society Symposium - Proceedings 604, 25.
Uchino, K., Zheng, J.H., Chen, Y.H., Du, X.H., Ryu, J., Gao, Y., Ural, S., Priya, S., Hirose, S., 2006. Loss mechanisms and high power piezoelectrics. Journal of Materials Science 41, 217.

Zhang, Q.M., Wang, H., Kim, N., Cross, L.E., 1994. Direct evaluation of domain-wall and intrinsic contributions to the dielectric and piezoelectric response and their temperature dependence on lead zirconate-titanate ceramics. Journal of Applied Physics 75, 454.